J. Opt. A: Pure Appl. Opt. **1** (1999) 477–482. Printed in the UK PII: S1464-4258(99)03575-8

Waveguidance by the photonic bandgap effect in optical fibres

Jes Broeng, Thomas Søndergaard, Stig E Barkou, Pablo M Barbeito and Anders Bjarklev

Center for Communications, Optics and Materials (COM), Technical University of Denmark, Building 348, DK-2800 Lyngby, Denmark

E-mail: jb@com.dtu.dk

Received 26 March 1999

Abstract. Photonic crystals form a new class of intriguing building blocks to be utilized in future optoelectronics and electromagnetics. One of the most exciting possibilities offered by photonic crystals is the realization of new types of electromagnetic waveguides. In the optical domain, the most mature technology for such photonic bandgap (PBG) waveguides is in optical fibre configurations. These new fibres can be classified in a fundamentally different way to all optical waveguides and possess radically different guiding properties due to PBG guidance, as opposed to guidance by total internal reflection. In this paper we summarize and review our theoretical work demonstrating the underlying physical principles of PBG guiding optical fibres and discuss some of their unique waveguiding properties.

Keywords: Optical fibres, photonic crystals, photonic bandgap, microstructural fibres

1. Introduction

Since the first proposals of a photonic bandgap (PBG) effect by Yablonovitch and John [1, 2], this subject has received a rapidly increasing research interest [3]. The fact that periodic dielectric structures may be designed to exhibit electromagnetic properties that bear a close resemblance to the electronic properties of semiconductors, is, naturally, of tremendous scientific interest [4]. Among the most interesting application-oriented prospects of PBG structures, or photonic crystals, are their ability to provide new means of waveguiding. By employment of the PBG effect as compared with the mechanism of total internal reflection (TIR), a completely new class of electromagnetic waveguides has emerged [5–7]. These waveguides possess properties fundamentally different to conventional TIR-based waveguides, including the remarkable ability to provide lossless transmission around 90° sharp bends [6]. Although not demonstrated at optical wavelengths, such lossless sharply bended waveguides were recently demonstrated experimentally at millimetre wavelengths in planar two-dimensional (2D) photonic crystal structures [8]. Due to the scalability of photonic crystals this result holds great promise for future realization of highly complex, all optical, integrated circuits. To fulfil the appealing prospects of high degrees of compactness and integration of optical circuitry using 2D photonic crystal structures, the major problem, at present, concerns achieving a good confinement in the third direction, i.e. in the direction perpendicular to the periodic plane. 2D photonic crystals are, naturally, intrinsically unable to provide this vertical confinement (an essential fact which is nonetheless neglected in most application-oriented 2D photonic crystal investigations). Due to this lack of vertical confinement and the finite height of real 2D photonic crystals, most fabricated PBG structures suffer from high losses [9]. Sandwiching a film of photonic crystal between two low-index material layers is not a sufficient requirement for obtaining leakage-free bound modes in the photonic film. Only under very precise conditions may such bound modes be obtained [10], making careful and detailed three-dimensional (3D) analysis and design of future planar PBG structures vital.

A second area where waveguiding by the PBG effect has been seen to break new ground is in the field of optical fibres [11]. In contrast to planar structures, optical fibres with a micron-scaled periodic arrangement of air holes in a silica background material may be readily fabricated [12]. As these fibres may be drawn to long lengths (using conventional optical fibre fabrication techniques), 2D photonic crystal of practically infinite height may be realized relatively easily, making optical fibres the most mature technology today for exploring PBG effects at optical wavelengths. Although silica–air photonic crystals do not exhibit PBGs for wave propagation refined strictly in the periodic plane, this system does allow for complete bandgaps (i.e. for any polarization of the light) to appear for waves propagating with a non-zero wavevector component in the direction perpendicular to the periodic plane [13]. This out-of-plane case is exactly the case of interest in optical fibres, where light is intended to be guided along the fibre axis.

First efforts into the realization of structures with a complete out-of-plane PBG for 2D silica–air photonic

1464-4258/99/040477+06$30.00

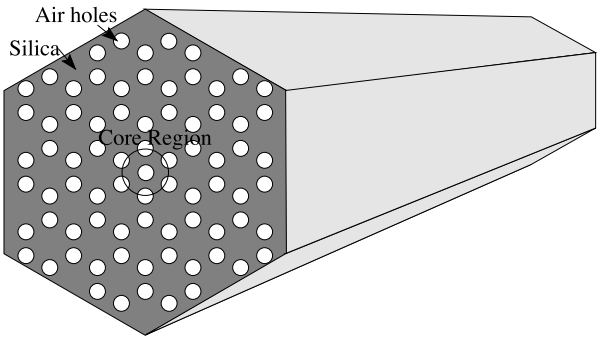

Figure 1. Cross-sectional schematic of honeycomb-based PCF.

crystals were performed using a triangular arrangement of air holes [11, 13]. This arrangement was predicted to exhibit complete bandgaps [13], but the requirement of large air hole sizes proved difficult to fulfil experimentally, and fabricated photonic crystal fibres (PCFs) using triangular arrangements of air holes showed no evidence of PBG effects (albeit other highly unusual properties are found for these index-guiding PCFs [14–16]). Our attention was, therefore, shifted to so-called honeycomb photonic crystals, which have been found to possess larger bandgaps than triangular crystals, both for in-plane and out-of-plane propagation [17, 18]. Theoretical results suggested that PCFs based on such honeycomb photonic crystal structures (see figure 1) would be able to exhibit waveguidance by PBG at realistic parameters [18], and their operation and basic properties were first described in [5, 19]. Recently these honeycomb-based low-index core PCFs were fabricated, and experimental results confirmed the theoretical predictions of PBG guidance [20]. In this paper, we outline the numerical tool used for the modelling of the PCFs, and elaborate on our theoretical work presented in [5, 18, 19].

In section 2, we present an efficient numerical method for modelling large photonic crystal structures. Improvements on silica–air honeycomb-based photonic crystals by using multiple silica dopants are presented in section 3. The principle of localization and guidance of light by the PBG effect is explained in section 4 along with a discussion of basic properties and future prospects of PBG guiding optical fibres.

2. Calculating PBG structures

In this section a variational method based on [21–24] for solving the vectorial magnetic-field wave equation for periodic structures is presented. The magnetic-field wave equation

$$\nabla \times \left(\frac{1}{\varepsilon_r(\boldsymbol{r})} \nabla \times \boldsymbol{H}(\boldsymbol{r}) \right) = \frac{\omega^2}{c^2} \boldsymbol{H}(\boldsymbol{r}), \tag{1}$$

is treated as an eigenvalue problem, where a solution $\boldsymbol{H}$ represents the eigenvector and $\frac{\omega^2}{c^2}$ is the corresponding eigenvalue. In the case of periodic structures a solution may, according to Bloch's theorem, be written as a plane wave modulated by a periodic function with the same periodicity as the structure. By approximating the periodic function with a Fourier-series expansion a solution may be written in the form

$$\boldsymbol{H}(\boldsymbol{r}) = \sum_{\boldsymbol{G}} \sum_{\lambda=1,2} \boldsymbol{h}_{\boldsymbol{k}+\boldsymbol{G},\lambda} \mathrm{e}^{\mathrm{i}(\boldsymbol{k}+\boldsymbol{G})\cdot\boldsymbol{r}}, \tag{2}$$

where $\boldsymbol{k}$ is a wavenumber vector, $\boldsymbol{G}$ is a reciprocal lattice vector and λ represents the two field directions perpendicular to $\boldsymbol{k} + \boldsymbol{G}$ (since $\nabla \cdot \boldsymbol{H} = 0$). The eigensolutions may be found using a variational method [3, 21, 23, 25] based on minimization of the functional

$$E(\boldsymbol{H}) = \frac{\langle \nabla \times \left(\frac{1}{\varepsilon_r(\boldsymbol{r})} \nabla \times \boldsymbol{H} \right) | \boldsymbol{H} \rangle}{\langle \boldsymbol{H} | \boldsymbol{H} \rangle}, \tag{3}$$

where

$$\langle \boldsymbol{F} | \boldsymbol{G} \rangle = \int \boldsymbol{F}^* \cdot \boldsymbol{G} \, \mathrm{d}^3 R. \tag{4}$$

When the functional $E(\boldsymbol{H})$ is at a minimum, $\boldsymbol{H}$ is an eigenvector and $E(\boldsymbol{H})$ is the corresponding eigenvalue $\frac{\omega^2}{c^2}$. By inserting a trial vector on the form (2) in (3) the functional effectively becomes a function of the coefficients $\boldsymbol{h}_{\boldsymbol{k}+\boldsymbol{G},\lambda}$, and the problem is reduced to varying the coefficients along a path that minimizes the functional $E(\boldsymbol{H})$. An efficient iterative method that performs this task is described in [23]. Higher-order eigensolutions are found by restricting the trial-vectors to being orthogonal to all previously found eigenvectors and using the same minimization principle. It is vital for the minimization approach that fast calculation of the left-hand side in (1) is performed. This is achieved by performing the rotations $\nabla\times$ in Fourier space, and the operation $\frac{1}{\varepsilon_r(\boldsymbol{r})}$ in real space. Fast Fourier transform (FFT) is used to go from one space to the other. Using this approach, however, interpolation of the dielectric function in real space is necessary to achieve good convergence. A method for interpolation based on effective medium theory [24] and a tensor representation of the dielectric constant is described in [21, 22].

In order to calculate the electromagnetic properties of a spatial defect within an otherwise periodic structure—such as the properties of the core region of the PCFs—the plane wave method may still be applied, where the smallest region describing the periodic structure is enlarged to include the defect (a so-called super-cell approximation). In this way a super-periodicity is introduced where the defect is also repeated periodically. Using a super-cell approximation the properties of the defect region may be accurately determined if the size of the super-cell is large enough to ensure that neighbouring defects are uncoupled. The numerical results presented in this paper have been calculated using the principles outlined in this section.

3. 2D honeycomb-based photonic crystals

The basic honeycomb structure is illustrated in figure 2, with an indication of the unit-cell of the structure. We denote the centre-to-centre distance between nearest air holes, Λ, and use this factor for the normalization of frequencies, as well as for the out-of-plane wavevector component, β, (i.e. the component in the invariant direction of the crystal). For a fixed β-value of $6/\Lambda$, the band structure diagram of a basic honeycomb structure with an air filling fraction of 30%

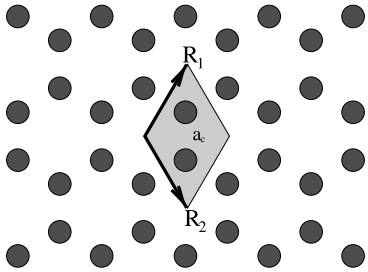

Figure 2. Basic 2D honeycomb photonic crystal structure. The periodicity of the structure is described through the two simple lattice vectors $\overline{R_1}$ and $\overline{R_2}$. The invariant direction is out of the paper.

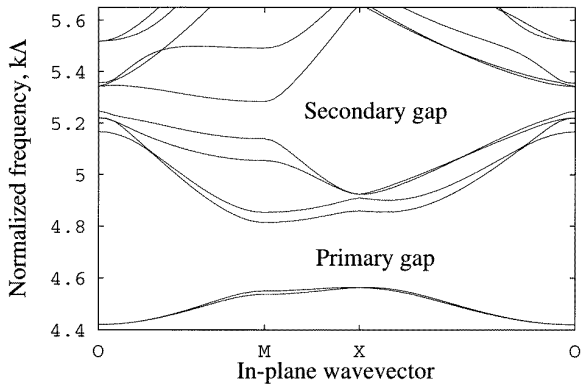

Figure 3. Band diagram for a basic honeycomb photonic crystal with an air filling fraction of 30%. $k\Lambda$ is the normalized frequency, where k is the free-space wavenumber ($= 2\pi/\lambda$). The three high-symmetry points of the honeycomb crystal are indicated by O, M and X.

is shown in figure 3. We assume the refractive index of undoped fused silica to be $n = 1.45$. From the figure we observe the appearance of two complete bandgaps: a primary gap between bands 2 and 3, and a secondary gap between bands 6 and 7. In order to increase the two bandgaps, we now focus on a strongly modified honeycomb-based optical lattice, where the effects of introducing several differently doped silica glasses is studied. Current doping technologies allow us to modify the dielectric constant of silica up to 3% and down to 1% of its nominal undoped value. A schematic of the structure is shown in figure 4, where the rhomboidal solid line represents the unit cell. The structure has a background material which comprises of interstitial holes and up to three different dopant levels of silica. The interstitial holes are easily introduced in a photonic crystal realized by the fabrication techniques currently used for PCFs [26]. These interstitial holes have already been demonstrated to be beneficial for the honeycomb structure, but to reduce the PBG effect in triangular structures [18]. In figure 5 the relative size of the primary gap is illustrated for the basic honeycomb structure with an air filling fraction of 30%. The relative bandgap size is defined as the difference between the upper and lower frequencies of the gap divided by its centre frequency. Although no PBGs exists for the in-plane case of silica–air structures ($\beta = 0$), complete PBGs are found to open up when moving out of the plane. The figure also includes three cases of modified honeycomb

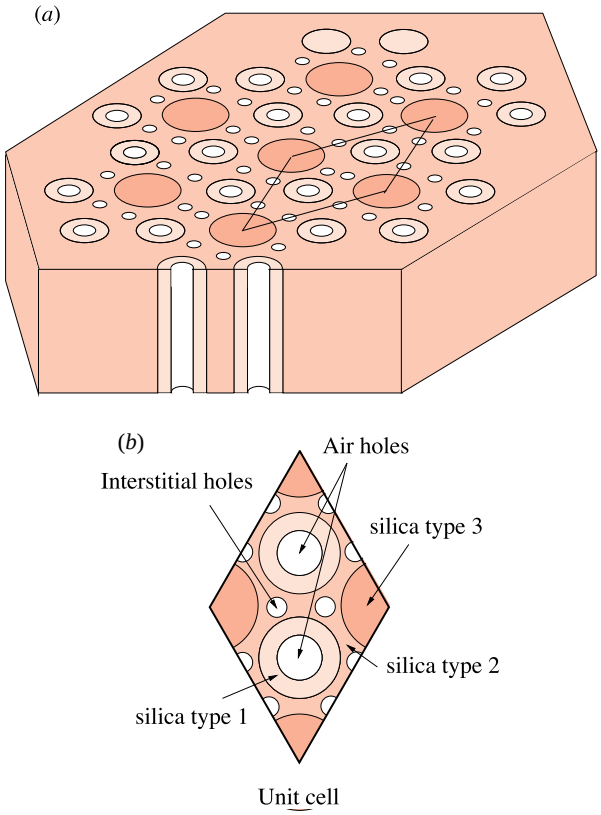

Figure 4. 2D modified honeycomb-based photonic crystal. Two differently doped silica glasses are used as well as undoped fused silica. The silica type 1 represents a capillary tube, and type 2 a solid cane from which the honeycomb silica–air photonic crystal may be fabricated. The unit cell of the structure is marked by the solid-line rhombus.

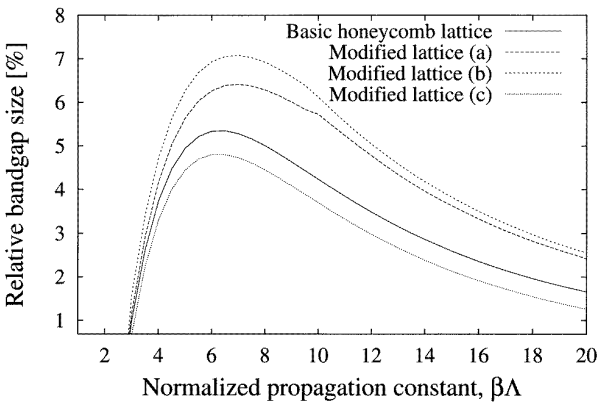

Figure 5. Relative bandgap size as a function of the normalized wave constant for the basic honeycomb lattice ($f = 30\%$), and three modified versions of the honeycomb lattice.

structures: (*a*) interstitial holes introduced ($f_{\text{int}} = 8\%$), (*b*) interstitial holes and three differently doped silica glasses ($n_1 = 1.44, n_2 = 1.45, n_3 = 1.47$), and (*c*) three differently doped silica glasses ($n_1 = 1.47, n_2 = 1.45, n_3 = 1.44$). The indices refer to the three silica types indicated in figure 4, and for the structures comprising three silica dopants the outer diameter of the tube and cane (silica types 1 and 3, respectively) have been set as large as possible ($= \Lambda$). For the basic structure (undoped silica and air) a maximum PBG

size of 5.3% at $\beta = 6.5/\Lambda$ is observed. This size may be increased to 6.4% by adding interstitial holes to the structure, and further increased to 7.1% by lowering the refractive index of the silica surrounding the air holes (silica type 1) while increasing the index of the silica forming the canes (silica type 3). By regarding the honeycomb photonic crystal as a structure with high-index nodes (the region with silica type 3) connected by bridging veins (the silica region between two air holes), we find that the results in figure 5 agree with the belief that increasing the node-index and narrowing the connecting veins is a fruitful route for designing large-bandgap photonic crystals [5]. To further support this, we observe how the size of the primary bandgap is, indeed, decreased for the structure (*c*) modified by lowering the index of the nodes, while increasing the index of the silica surrounding the air holes. Although not illustrated here, we found the same conclusions also to be valid for the size of the secondary bandgap. This result demonstrates the advantages of introducing differently doped silica glasses in the honeycomb-based photonic crystal.

4. Waveguidance by the PBG effect

By locally breaking the periodicity of a photonic crystal, a spatial region with optical properties different from the surrounding bulk photonic crystal can be created. If such a defect region supports modes with frequencies falling inside the forbidden gap of the surrounding full-periodic crystal, these modes will be strongly confined to the defect. This is the principle on which the operation of the PBG guiding fibres relies, namely a complete out-of-plane 2D bandgap exhibited by the photonic crystal cladding, and a correctly designed defect, forming a spatial region to which very strong transverse confinement can be achieved. For this defect region to exhibit optical properties different from the surrounding periodic structure (i.e., be able to support a localized mode) it is important to notice that it is not a requirement that the defect region has a higher index than its surroundings. For a homogeneous dielectric surrounding media this would be the only case under which localization can occur (which is, of course, the case of TIR utilized in all conventional optical waveguides). Leakage-free guidance of light confined to a region with a lower index than its surroundings would, therefore, not be expected to be possible from index guidance waveguide theory, but if the surrounding material exhibits PBG effects even a low-index defect region may be able to localize the light, and thereby act as a (new) highly unusual waveguide. In the following, we will be more specific in our description of the PBG guiding fibres and illustrate the influence of introducing a defect in the full-periodic honeycomb structure. In figure 6 we have depicted the bandgaps for the primary and secondary bandgap of the honeycomb PCF shown in figure 1 with a cladding air filling fraction of 10% and a defect hole with the same size as the cladding holes. Inside the primary gap, we observed a single defect-mode traversing the gap from $\beta\Lambda \approx 5$ to $\approx$17. This mode is caused solely by the introduction of the defect air hole in the honeycomb structure. For the full periodic structure, we find exactly the same PBGs (with no modes inside) with identical boundaries to those of the crystal including

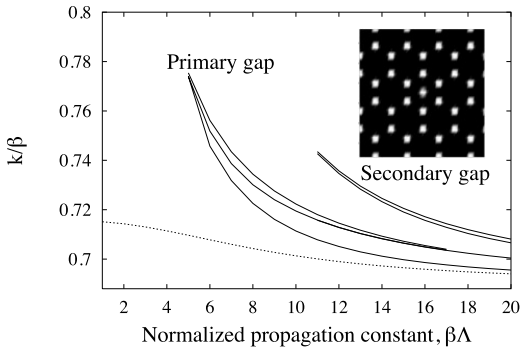

Figure 6. Illustration of the two first bandgaps (primary and secondary gaps) of a honeycomb PCF with a cladding air filling fraction of 10% and a defect hole with same size as the cladding holes. Within the primary bandgap the extra air hole in the core of the fibre causes a single degenerate mode to appear. This 'defect' mode is localized around the core of the fibre, and does not couple to the cladding structure (as it is here forbidden due to the PBG effect). The field distribution of the core mode is illustrated in figure 7. For a fibre with $\Lambda = 2.0$ μm the core mode falls within the primary bandgap in a wavelength range which corresponds approximately to 1.0–3.0 μm. Leakage-free, single-mode waveguidance is thus obtained over this wavelength range. The dotted curve relates to the effective index of the cladding structure. 16 384 plane waves were used for the calculation.

the defect. We expect this defect mode to be strongly localized to the region comprising the extra air hole (albeit this is a low-index region), and have in figure 7 illustrated its calculated squared amplitude of the E-field. The mode was calculated for a $\beta\Lambda$ value of 8.0. For this value, the defect mode is approximately in the middle of the bandgap, and the expected strong localization of the mode is apparent. This mode does not couple to cladding modes in the PCF, (since the mode is falling inside the bandgap of the photonic crystal cladding) and lossless guidance may therefore, in principle, be achieved over long lengths. Although almost all of the field of the defect mode for this particular PCF is distributed in the silica, full confinement of light in air is—in principle—possible for PBG guiding fibres. Using the illustration of figure 6, this requires a defect mode falling inside a bandgap, where both extend to $k\beta \geqslant 1$ (i.e. crossing the air line). Such fibres would, naturally, have a tremendous potential in both telecommunications and sensor areas. Also included in figure 6 is the radiation line (dotted curve), defined as the lowest frequency allowed mode in the full periodic structure—and relates to the effective index, $n_{\mathrm{eff,cladding}}$, of the cladding structure as $1/n_{\mathrm{eff,cladding}}$. Below this line is a semi-infinite 'bandgap', where no modes exist. This is the region in which all TIR-based fibres (including triangular PCFs [12]) operate, since a high-index defect causes at least one mode to appear below this line. Such index-guided modes are seen not to be a feature of the low-index core honeycomb-based PCFs.

For comparison with the (realistic) PCF having $f = 10\%$, in figure 8 we have illustrated the modes of a honeycomb PCF with $f = 30\%$, and a defect hole size also corresponding to $f = 30\%$. Remarkable is the fact that the defect mode for this PCF configuration does not fall inside the primary bandgap, but in the secondary. The gaps are, however, much wider for the PCF with $f = 30\%$, giving a

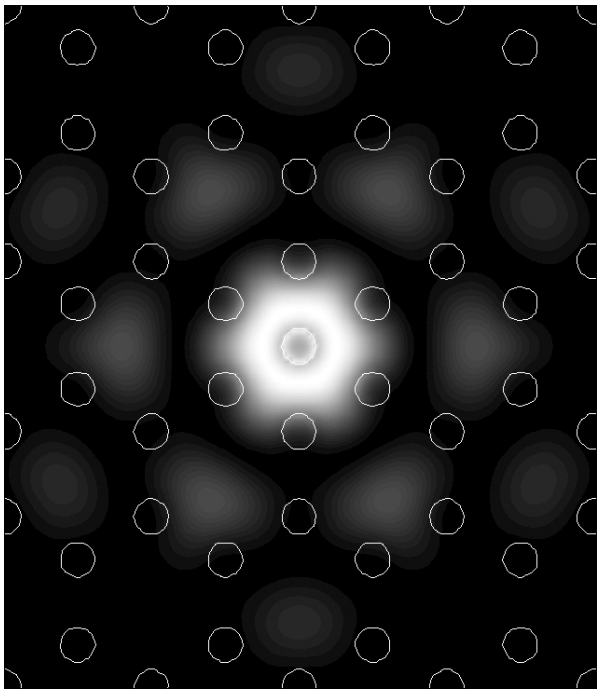

Figure 7. PBG guided mode for a honeycomb PCF with $f = 10\%$. The figure shows the electric field squared for the 'defect' mode illustrated in figure 6. Light areas indicate high field intensity. The real-space structure has been superimposed to illustrate the localization of the 'defect' mode to the extra air hole in the core of the fibre.

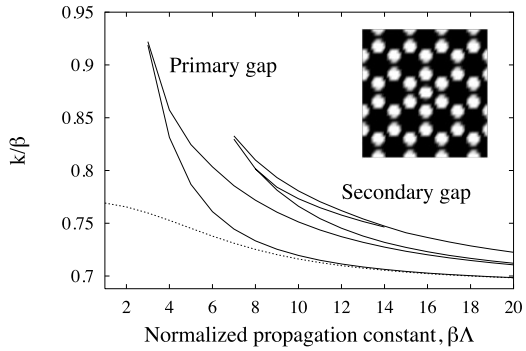

Figure 8. Illustration of defect mode falling inside the secondary bandgap for a honeycomb PCF with a cladding air filling fraction of 30% and a defect hole with same size as the cladding holes.

wider range for 'tuning' the properties of the guided mode. For $\Lambda = 2.0$ μm the mode in figure 8 is guided from 1.3–2.2 μm. Whereas for a PCF with the same cladding air filling fraction, but a much smaller defect hole, corresponding to $f = 10\%$, a defect mode was found in the primary gap, and guided (as the only defect mode) over a wavelength range as large as 1–3.0 μm for $\Lambda = 2.0$ μm. For a larger defect air hole, corresponding to $f = 60\%$ no defect modes were found neither in the primary gap nor in the secondary. Since real 2D PBG structure do not extend infinitely in the periodic plane, the size of the bandgaps will be of importance for the performance of PBG guiding fibres in practical applications. Larger bandgaps mean a stronger confinement of the defect mode, and will, therefore, not only be of importance for wider 'tuning'-ranges of the fibres, but

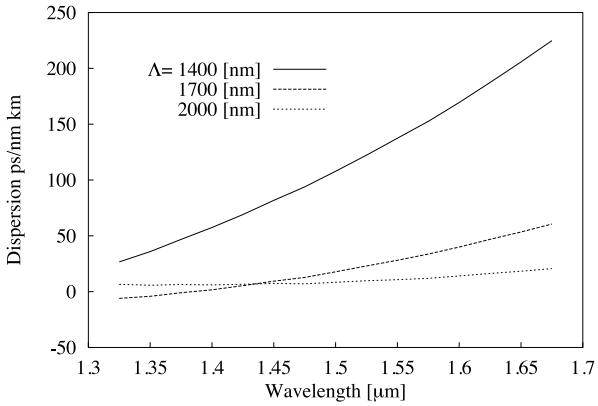

Figure 9. Dispersion of the PBG guiding PCF. The material dispersion of silica is included through the Sellmeier dispersion relation. Similar results are presented in [27].

also for very robust operation of these with respect to low propagation and bending losses. Although here we have not elaborated on honeycomb PCFs having improved cladding structures, as those investigated in section 3. We will, in future work, be addressing such improved PCFs.

The dispersive properties in the bandgap guiding PCFs is an important issue, where the novel guidance mechanism may provide optical components with characteristics unlike any others. To investigate this, we have calculated the dispersion, $D = -\frac{\lambda}{c}\frac{\mathrm{d}^2 n}{\mathrm{d}\lambda^2}$ for a honeycomb PCF with $f = 18\%$ and a defect hole size corresponding to $f = 7\%$ for a series of Λ values (see figure 9). To include the material dispersion in the calculations, we used an iterative scheme to account for the wavelength dependence of the refractive index of silica. From figure 9 it is noted that the dispersion can be increased significantly above the material dispersion, an unusual feature for a single-mode fibre. To be specific $D \approx 150$ ps nm^{-1} km^{-1} is found at 1.55 μm for $\Lambda = 1400$ nm. Another important feature is found for $\Lambda = 2000$ nm, namely a very flat dispersion around 1.55 μm. Looking at the value of λ with near-zero dispersion, we notice that PBG-guiding PCFs appear to make it possible to have fibres with a dispersion arbitrarily close to zero at a desired wavelength.

5. Summary

In this paper we have addressed the physical principle behind waveguidance by the PBG effect in dielectric waveguides. We have outlined the theoretical tools currently used for the modelling of PCFs, and basic properties of bandgap guiding PCFs have been discussed. Larger bandgaps were found for realistic honeycomb-based photonic crystal cladding structures, where the optical lattice was modified by including several differently doped silica glasses as well as small interstitial air holes. For PBG-guiding fibres to become standard components in future optical systems, such improvements may be of significant importance, resulting in very robust operation through low propagation and bending losses. Finally, the dispersive properties of bandgap-guiding fibres were investigated, and as a completely novel quality we found the fibres were able to exhibit very large positive dispersion for single-mode operation. This might be utilized

for dispersion management in fibre systems with negative dispersion. Another important dispersion feature was found for fibres with similar geometry as the large-dispersion fibres, but fabricated at larger dimensions, namely a very flat near-zero dispersion over a very broad wavelength range. Although the research in PBG-guiding fibres is still in its infancy, and important issues must be addressed such as e.g. drawing long, uniform, low-loss lengths of the fibres, their potential as ultralow-loss transmission fibres, as well as their dispersive properties may pave the way for PBG fibres to become of commercial interest in optical communications.

Acknowledgment

This work was supported by the Danish Technical Research Council under the THOR (Technology by Highly Oriented Research) programme.

References

[1] Yablonovitch E 1987 Inhibited spontaneous emission in solid-state physics and electronics *Phys. Rev. Lett.* **58** 2059–62

[2] John S 1987 Strong localization of photons in certain disordered dielectric superlattices *Phys. Rev. Lett.* **58** 2486–9

[3] Joannopoulos J D, Winn J N and Meade R D 1995 *Photonic Crystals: Molding the Flow of Light* (Princeton, NJ: Princeton University Press)

[4] See e.g. Rarity J and Weisbuch C 1996 *Microcavities and PBGs Physics and applications (NATO ASI Series. Series E, Applied Sciences vol 324)* (Dordrecht: Kluwer)

[5] Broeng J, Mogilevtsev D, Barkou S E and Bjarklev A 1999 Photonic crystal fibres: a new class of optical waveguides *Opt. Fiber Technol.* at press

[6] Mekis A, Chen J C, Kurland I, Fan S, Villeneuve P R and Joannopoulos J D 1996 High transmission through sharp bends in photonic crystal waveguides *Phys. Rev. Lett.* **77** 3787–90

[7] Benisty H 1996 Modal analysis of optical guides with two-dimensional photonic band-gap boundaries *J. Appl. Phys.* **79** 7483–92

[8] Lin S-Y, Chow E, Hietala V, Villeneuve P R and Joannopoulos J D 1998 Experimental demonstration of guiding and bending of electromagnetic waves in a photonic crystal *Science* **282** 274–6

[9] Krauss T F, De La Rue R M and Brand S 1996 Two-dimensional photonic-bandgap structures operating at near-infrared wavelengths *Nature* **383** 699–702

[10] Russell P St J, Pottage J, Broeng J, Mogilevtsev D and Philips P L 1999 Leak-free bound modes in photonic crystal films *CLEO'99: Conf. on Lasers and Electro-optics (Baltimore, 25–27 May 1999)* submitted

[11] Knight J C, Birks T A, Russell P St J and Atkin D M 1996 All-silica single-mode optical fibre with photonic crystal cladding *Opt. Lett.* **21** 1547–9

[12] Knight J C, Birks T A, Russell P St J and Sandro J P 1998 Properties of photonic crystal fibre and the effective index model *J. Opt. Soc. Am.* A **15** 748–52

[13] Birks T A, Roberts P J, Russell P St J, Atkin D M and Shepherd T J 1995 Full 2-D PBGs in silica/air structures *Electron. Lett.* **31** 1941–3

[14] Birks T A, Knight J C and Russell P St J 1997 Endlessly single-mode photonic crystal fibre *Opt. Lett.* **22** 961–3

[15] Bjarklev A, Broeng J, Barkou S E and Dridi K 1998 Dispersion properties of photonic crystal fibres *Eur. Conf. on Optical Communications (Madrid, September 20–24)* pp 135–6

[16] Mogilevtsev D, Birks T A and Russell P St J 1998 Group velocity dispersion in photonic crystal fibres *Opt. Lett.* **23** 1662–4

[17] Cassagne D, Jouanin C and Bertho D 1996 Hexagonal photonic-band-gap structures *Phys. Rev.* B **53** 7134–42

[18] Broeng J, Barkou S E, Bjarklev A, Knight J C, Birks T A and Russell P St J 1998 Highly increased photonic band gaps in silica/air structures *Opt. Commun.* **156** 240–4

[19] Barkou S E, Broeng J and Bjarklev A 1999 Silica/air photonic crystal fibre design that permits waveguiding by a true photonic bandgap effect *Opt. Lett.* **24** 46–8

[20] Knight J C, Broeng J, Birks T A and Russell P St J 1998 Photonic band gap guidance in optical fibres *Science* **282** 1476–8

[21] Meade R D, Rappe A M, Brommer K D, Joannopoulos J D and Alerhand O L 1993 Accurate theoretical analysis of photonic band-gap materials *Phys. Rev.* B **48** 8434–7

[22] Meade R D, Rappe A M, Brommer K D, Joannopoulos J D and Alerhand O L 1997 Accurate theoretical analysis of photonic band-gap materials *Phys. Rev.* B **55** 15 942 (erratum)

[23] Teter M P, Payne M C and Allan D C 1989 Solution of Schrödinger's equation for large systems *Phys. Rev.* B

[24] Aspnes D E 1981 Local-field effects and effective-medium theory: A microscopic perspective *Am. J. Phys.* **50** 704–9

[25] Bransden B H and Joachain C J 1989 *Introduction to Quantum Mechanics* (Harlow: Longman)

[26] Knight J C, Birks T A, Cregan R F and Russell P St J 1999 Photonic crystals as optical fibres—physics and applications *Opt. Mater.* **11** 143–51

[27] Barkou S E, Broeng J and Bjarklev A 1999 Dispersion properties of PBG guiding fibres *Optical Fiber Communication Conf. (San Diego, CA, February 1999)* p FG5